
Article

Climate Change will Weaken the Ability of Natural Enemies to Control the Asian Longhorned Beetle, *Anoplophora glabripennis* (Coleoptera: Cerambycidae)

Quan-Cheng Zhang, Jun-Gang Wang* and Yong-Hui Lei

College of Agriculture, Shihezi University, Shihezi 832003, China

* Correspondence: wangjungang98@163.com; Tel.: +86-13289937169.

Simple Summary: The Asian longhorned beetle, *Anoplophora glabripennis* is a worldwide invasive creature that has invaded the world for more than 20 years. Although previous studies have predicted the distribution range of *Anoplophora glabripennis*, this single species distribution prediction cannot provide more potential management strategies for the control of invasive organisms. In this study, we incorporated two important natural enemies (*Dastarcus helophoroides* and *Dendrocopos major*) of *Anoplophora glabripennis* into the prediction model. And assess the ability of natural enemies to control *Anoplophora glabripennis* under future climate change conditions. We found that Climate changing led to the northward migration of the suitable areas of *Anoplophora glabripennis* and its natural enemies. However, the northward migration of the *Dastarcus helophoroides* and *Dendrocopos major* cannot catch up with the northward migration of *Anoplophora glabripennis*. Therefore, the change of climate weakened the ability of natural enemies to control the *Anoplophora glabripennis*. Due to the lack of natural enemies in the new intruded areas, *Anoplophora glabripennis* may cause greater damage in future climatic conditions. The research will provide new insights and potential management strategies for invasive management of pests.

Abstract: The Asian longhorned beetle (ALB), *Anoplophora glabripennis* is a forestry pest found worldwide. ALB causes serious harm because of the lack of natural enemies in the invaded areas. *Dastarcus helophoroides* and *Dendrocopos major* are important natural enemies of ALB. MaxEnt was used to simulate the distribution of *D. helophoroides* and *D. major* in China and Xinjiang, and their suitable areas were superimposed to evaluate the pest control ability of *D. helophoroides* and *D. major*. The results showed that, with climate change, the suitable areas of *D. helophoroides* and *D. major* migrated northward; the centroid shift of ALB was greater than that of *D. helophoroides* and *D. major*, which would lead to fewer natural enemies encountered by ALB during migration, reduce the control ability of natural enemies, and increase the risk of disastrous outbreaks in the invaded areas. We found that the damage caused by ALB was not serious in the areas with natural enemies and very serious in the areas without natural enemies. We suggest that natural enemies should be included in the model used for predicting suitable areas for invasive pests, as this is more conducive to assessing the risks of invasive organisms to the local ecological environment.

Keywords: *Anoplophora glabripennis*; *Dastarcus helophoroides*; *Dendrocopos major*; MaxEnt; climate change; natural enemy; pest management

1. Introduction

The Asian longhorned beetle (ALB), *Anoplophora glabripennis*, has strong invasiveness and destructive power as an important forestry pest [1]. It originated in China and Korea [2], and it has a wide range of host plant species, including more than 15 genera such as *Ulmus*, *Populus*, *Salix*, and *Acer* that are continuously infected by ALB [3]. Since 1996, ALB has been found worldwide [4]; it has successively invaded the United States (1996) [4], Austria (2001) [5], Canada (2003) [6], France (2003), Germany (2004), Italy (2007),

Belgium (2008), the Netherlands (2010), Switzerland (2011), the United Kingdom (2012), Finland (2015), and Montenegro (2015) [7]. In addition, ALB has been found and invaded for more than 20 years in Xinjiang, China [8]. ALB poses significant management risks to invaded cities, farmland, forests, and ecosystems [9].

Although ALB adults are relatively large, the eggs, larvae, and pupae are easily hidden in logs and boxes for transmission [10]. It is by virtue of this concealment that ALB has invaded the world for more than 20 years [4]. Because ALB hosts are widely distributed, there are host species of ALB in almost all countries or regions [3]. ALB can rely on these hosts to establish new populations, and it is very difficult to completely eradicate ALB [1]. Of course, successful cases of eradication have been reported. For example, it took 11 years to completely eradicate ALB in the Cornuda region of northeast Italy [11]. However, it is difficult to eradicate ALB completely in all invaded areas, especially because it takes a long time to eradicate a large number of trees [1]. We began to think of a sustained, natural, low-cost way of controlling ALB. According to the classical biological control theory, more valuable natural enemies can be selected from the area of origin and introduced into the invaded area to control the pest population [12-13]. The latitude range of the ALB invasion area is similar to that of the distribution area at the origin, which provides feasibility for introducing natural enemies from the area of origin to control the damage of ALB in the invasion area [14].

Generally, it is difficult for invasive organisms to find natural enemies in new environments [15]. The invasive organisms can reproduce, survive, and occupy ecological sites rapidly [16]. We tried to find potential predators for these ALB-invaded areas. We reviewed important natural enemies of ALB in the local environment. In China, *Dastarcus helophoroides* and *Dendrocopos major* are two important natural enemies of ALB [14,17]. *D. helophoroides*, a parasitic beetle, has a control effect of 63–76% on mature ALB larvae and pupae [18]. *D. major*, an important predatory natural enemy of ALB, can prey on 22% of ALB larvae in trunks [19]. ALB may be controlled by releasing *D. helophoroides* and attracting *D. major* [19-20].

MaxEnt is a species distribution prediction model based on the maximum entropy theory [21]. The MaxEnt model is suitable for studies of biological invasions and responses to climate change [22] because its accuracy is better than that of other models and it is easy to use. Previous studies have predicted the distribution of ALB in Europe [23], North America [24], Massachusetts [25], eastern Canada [26], and worldwide [27-28]. However, these studies did not analyze natural enemy factors and did not evaluate whether there are any natural enemy resources that can naturally control ALB in the invaded regions.

Currently, prediction of species distribution with the niche model is basically used for single species, especially for invasive pests. When we analyze the potential distribution areas of these species, we often ignore whether there are any natural enemy resources suitable for control in the invaded areas. These analyses cannot play a more positive role in the invasion management of pests. Therefore, we believe that the distribution of natural enemies in their natural environment needs to be considered during the analyses of invasive species, to effectively evaluate the risk of pests worldwide and positively contribute to the risk management of pests.

In this study, we used the MaxEnt model, in combination with climatic factors and topographic conditions, to predict the suitable areas of ALB in China and Xinjiang. Simultaneously, we selected important natural enemies of ALB, *D. helophoroides* and *D. major*, as cases to predict and analyze the suitable areas of these two natural enemies in China and Xinjiang. Finally, we evaluated the ability of *D. helophoroides* and *D. major* to control ALB against the background of climate change. Our research will positively contribute to the risk management of invasive pests.

2. Materials and Methods

2.1. Distribution point collection

According to the literature, news reports, and various forestry pest quarantine websites (e.g., CABI, GBIF, recorded data of other institutions, and related literature reports), the distribution points of ALB, *D. helophoroides*, and *D. major* in China were recorded. The longitude and latitude were located using Google Earth (international common geographic coordinate system). The rotation minute-second was in the decimal format, and the longitude and latitude were recorded. A total of 101 occurrence points were saved in the csv format, which conforms to MaxEnt model input data (Figure 1).

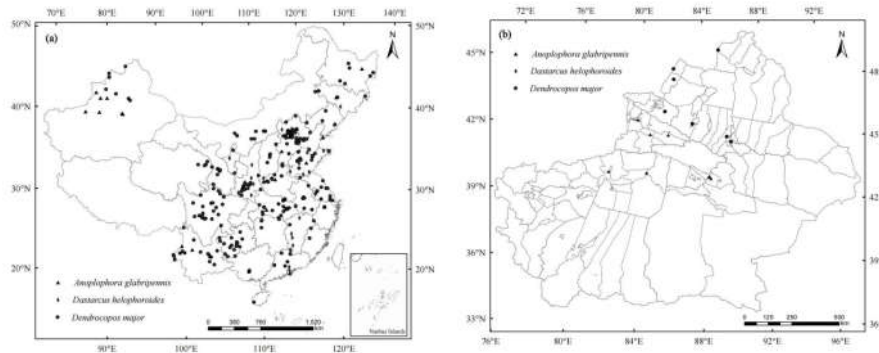


Figure 1. Known geographical distribution of *Anoplophora glabripennis*, *Dastarcus helophoroides*, and *Dendrocopos major* in (a) China and (b) Xinjiang.

2.2. Climate data collection and environmental variables

The climate data in this study come from the WorldClim database (<https://www.worldclim.org/>), which contains 19 variables (Table S1) [29]. We selected the 1970-2000 climate data as the current climate. The latest WorldClim version 2.1 (<https://worldclim.org/>) was used to obtain projected future climate data. We selected 4 types of global climate models (GCMs) and 3 types of Shared Socio-economic Pathways (SSPs) [30]. GCMs include BCC-CSM2-MR, CanESM5, CNRM-CM6-1, MIROC6. SSPs include SSP126 (low greenhouse gas emissions), SSP245 (medium greenhouse gas emissions), and SSP585 (high greenhouse gas emissions). The projected future periods are 2041-2060 and 2081-2100, which represent the middle and end of this century, respectively. In total, we have taken into consideration 24 future climatic scenarios. In addition to bioclimatic variables, we also considered terrain, including elevation, slope and aspect [31]. We downloaded the elevation data from the Geospatial Data Cloud (<http://www.gscloud.cn/>), and used the software ArcGIS version 10.4.1 (<https://www.arcgis.com/>) to obtain the aspect and slope data. The spatial resolution of all variables was 30-s, and ArcGIS version 10.4.1 was used to obtain China-wide data.

In order to reduce the multicollinearity among the environment variables, we used the ENMTools.pl software to analyze the correlation of candidate variables (including 19 bioclimatic variables and 3 terrain variables [32]). We define the Pearson correlation coefficient of 0.8 as the threshold to determine whether we should remove particular highly-correlated variables [33]. Therefore, we selected Bio1, Bio2, Bio4, Bio10, Bio12, Bio14, Bio15, Bio20, Bio21, Bio22 as the environmental variables of ALB distribution model (Table S2). Bio1, Bio3, Bio4, Bio6, Bio11, Bio12, Bio13, Bio19, Bio20 and Bio21 were selected as the environmental variables for constructing the distribution model of *D. helophoroides* (Table S3). Selected Bio3, Bio4, Bio6, Bio11, Bio12, Bio15, Bio16, Bio19, Bio21, Bio22 as the environment variables of *D. major* distribution model (Table S4).

2.3. Optimization of model parameters

Load the Kuenm package (<https://github.com/marloncobos/kuenm>) with R version 3.6.3 (<https://www.r-project.org/>) to optimize two important parameters in MaxEnt : feature class (FC) and regularized multiplier (RM) [34]. In this study, we set the RM value to 0.1-4, each increase 0.1. Using Akaike information criterion correction (AICc) to evaluate the fitting degree and complexity of different parameter combinations [35]. Statistical significance (partial ROC) was used. The area under receiver operating characteristic curve (AUC) was used to evaluate the ability of different parameter combinations to distinguish test points and background points [36]. The difference between training and testing AUC, 10% training omission rate and minimum training presence omission rate were used to evaluate the fitting degree of different parameter combinations, and the most suitable parameter combination [36]. The relative contribution of each environmental variable was evaluated by using the Jackknife test [37-38].

2.4. Change of suitable area under different climate

The simulation results use SDMtool tool to calculate the distribution centroid and area changes in different periods of scenarios [39]. ArcGIS software is used to load SDMtoolbox toolkit. After loading successfully, the prediction results of ALB, *D. helophoroides*, and *D. major* in different periods are converted into binary grid files by ArcGIS software and SDMtools toolkit. Then select the 'Universal Tools' subdirectory 'Distribution Changes Between Binary SDMs' tool in the 'SDMTools' module to calculate the expansion area, stability area and contraction area of ALB, *D. helophoroides*, and *D. major* suitability area under different periods of scenarios. The 'Centroid Changes (Line)' tool was used to calculate the geometric center displacement of the predicted distribution in different periods, and the overall change trend of ALB, *D. helophoroides*, and *D. major* suitable areas was detected.

3. Results

3.1. Potential suitable areas for ALB, *D. helophoroides*, and *D. major* under current and future climate conditions

Currently, unsuitable area, lowly suitable area, moderately suitable area, and most suitable area for ALB in China account for 86.79%, 8.99%, 3.14%, and 1.09%, respectively (**Figure 2a; Figure S1a**). By 2050, the percentages of unsuitable area, lowly suitable area, moderately suitable area, and most suitable area would be 82.66%, 10.55%, 4.69%, and 2.11%, respectively (**Figure 2b; Figure S1b**). By 2090, the percentages of unsuitable area, lowly suitable area, moderately suitable area, and most suitable area would be 81.76%, 11.50%, 4.52%, and 2.22%, respectively (**Figure 2c; Figure S1c**). Currently, the percentages of unsuitable area, lowly suitable area, moderately suitable area, and most suitable area for ALB in Xinjiang are 88.47%, 6.95%, 3.25%, and 1.33%, respectively (**Figure 3a; Figure S1d**). By 2050, the percentages of unsuitable area, lowly suitable area, moderately suitable area, and most suitable area would be 78.66%, 11.44%, 6.50%, and 3.40%, respectively (**Figure 3b; Figure S1e**). By 2090, the percentages of unsuitable area, lowly suitable area, moderately suitable area, and most suitable area would be 75.77%, 11.88%, 7.55%, and 4.79%, respectively (**Figure 3c; Figure S1f**).

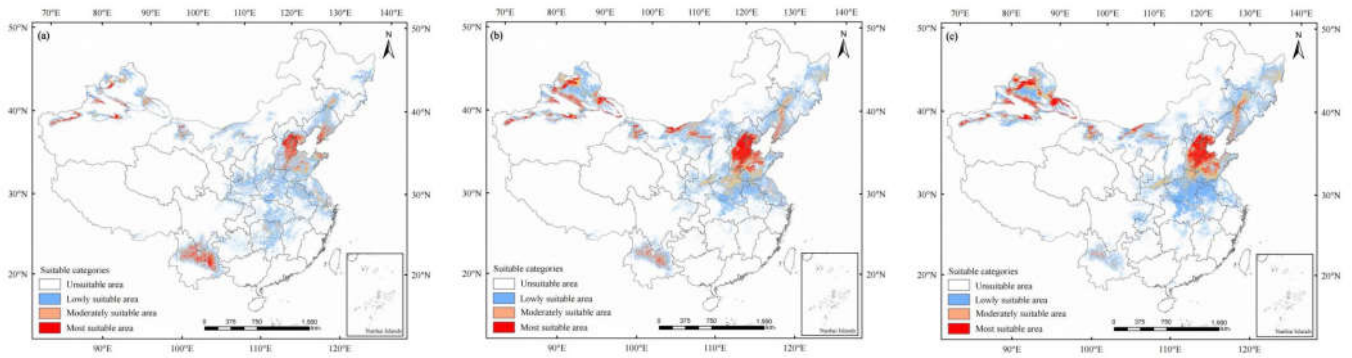


Figure 2. Potential distribution of *Anoplophora glabripennis* in China predicted using the MaxEnt model under (a) the current climate and according to climate change in (b) 2050 and (c) 2090.

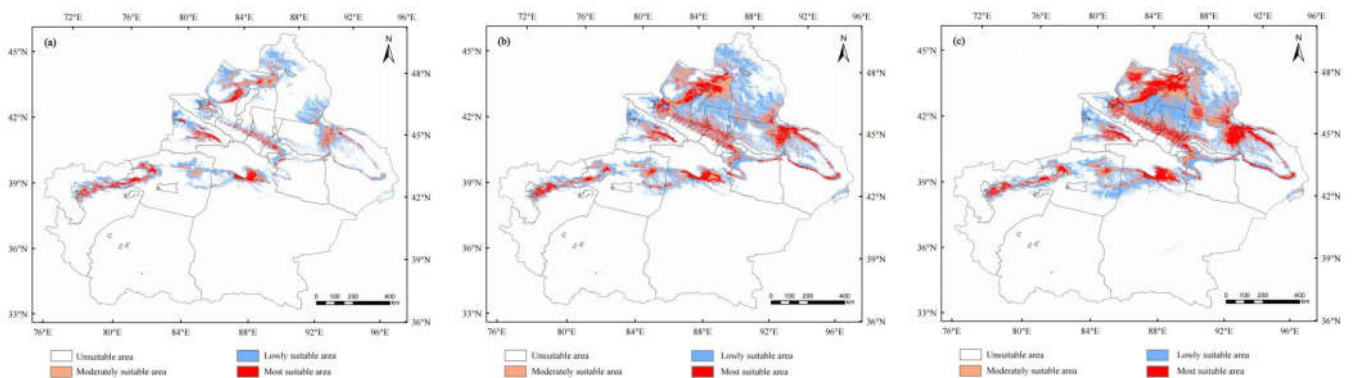


Figure 3. Potential distribution of *Anoplophora glabripennis* in Xinjiang predicted using the MaxEnt model under (a) the current climate and according to climate change in (b) 2050 and (c) 2090.

Currently, the percentages of unsuitable area, lowly suitable area, moderately suitable area, and most suitable area for *D. helophoroides* in China are 49.22%, 20.34%, 13.17% and 17.27%, respectively (**Figure 4a; Figure S2a**). By 2050, the percentages of unsuitable area, lowly suitable area, moderately suitable area, and most suitable area would be 38.68%, 24.67%, 18.84%, and 17.81%, respectively (**Figure 4b; Figure S2b**). By 2090, the percentages of unsuitable area, lowly suitable area, moderately suitable area, and most suitable area would be 36.47%, 25.02%, 20.28%, and 18.23%, respectively (**Figure 4c; Figure S2c**). Currently, the percentages of unsuitable area, lowly suitable area, moderately suitable area, and most suitable area for *D. helophoroides* in Xinjiang are 67.94%, 31.88%, 0.18%, and 0.00%, respectively (**Figure 5a; Figure S2d**). By 2050, the percentages of unsuitable area, lowly suitable area, moderately suitable area, and most suitable area would be 42.33%, 55.39%, 2.28%, and 0.00%, respectively (**Figure 5b; Figure S2e**). By 2090, the percentages of unsuitable area, lowly suitable area, moderately suitable area, and most suitable area would be 37.83%, 56.57%, 5.59%, and 0.01%, respectively (**Figure 5c; Figure S2f**).

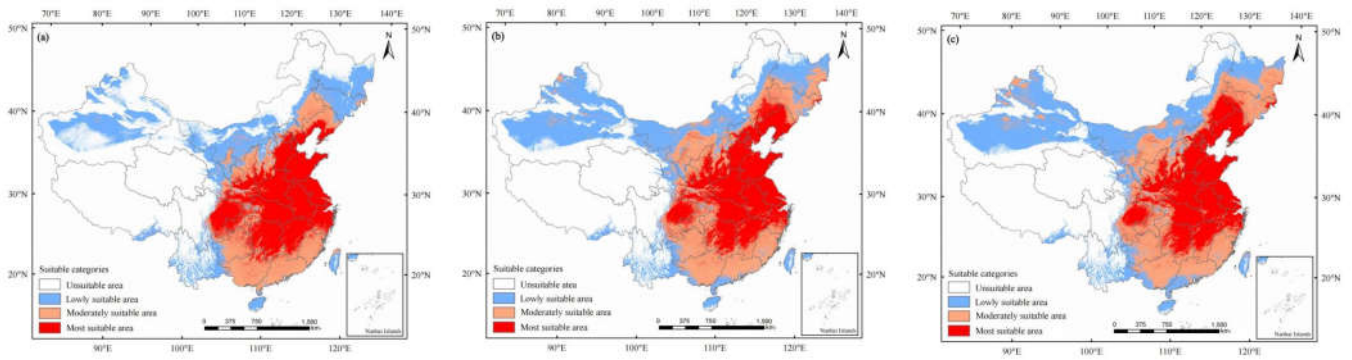


Figure 4. Potential distribution of *Dastarcus helophoroides* in China predicted using the MaxEnt model under (a) the current climate and according to climate change in (b) 2050 and (c) 2090.

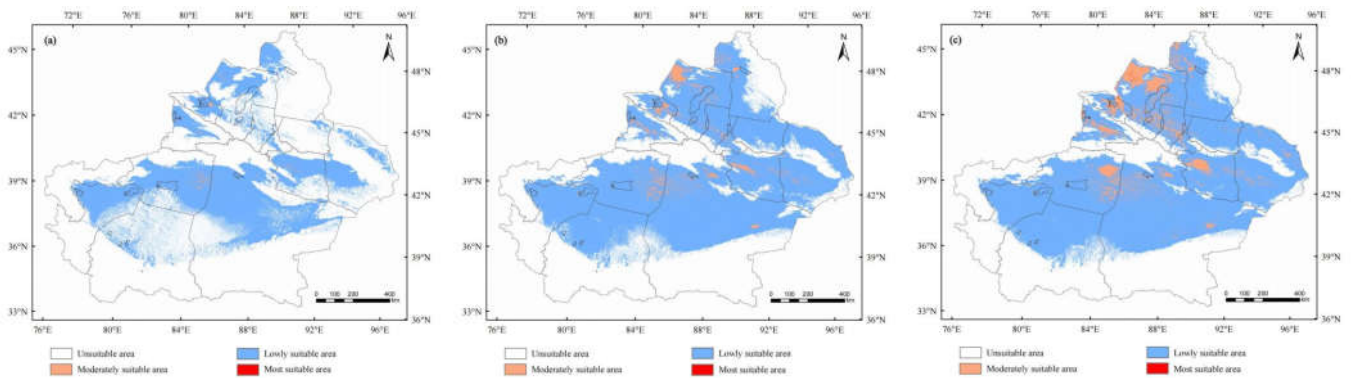


Figure 5. Potential distribution of *Dastarcus helophoroides* in Xinjiang predicted using the MaxEnt model under (a) the current climate and according to climate change in (b) 2050 and (c) 2090.

Currently, the percentages of unsuitable area, lowly suitable area, moderately suitable area, and most suitable area for *D. major* in China are 42.81%, 24.85%, 19.94%, and 12.39%, respectively (**Figure 6a**; **Figure S3a**). By 2050, the percentages of unsuitable area, lowly suitable area, moderately suitable area, and most suitable area would be 31.29%, 32.70%, 26.64%, and 9.37%, respectively (**Figure 6b**; **Figure S3b**). By 2090, the percentages of unsuitable area, lowly suitable area, moderately suitable area, and most suitable area would be 28.90%, 38.89%, 24.95%, and 7.26%, respectively (**Figure 6c**; **Figure S3c**). Currently, the percentages of unsuitable area, lowly suitable area, moderately suitable area, and most suitable area for *D. major* in Xinjiang are 81.65%, 18.30%, 0.05%, and 0.00%, respectively (**Figure 7a**; **Figure S3d**). By 2050, the percentages of unsuitable area, lowly suitable area, moderately suitable area, and most suitable area would be 51.58%, 48.10%, 0.31%, and 0.00%, respectively (**Figure 7b**; **Figure S3e**). By 2090, the percentages of unsuitable area, lowly suitable area, moderately suitable area, and most suitable area would be 44.95%, 54.51%, 0.54%, and 0.00%, respectively (**Figure 7c**; **Figure S3f**).

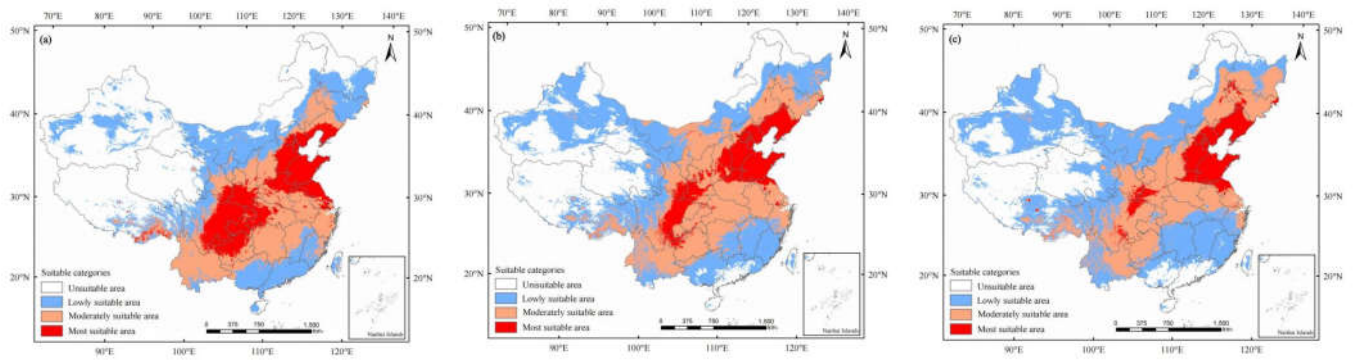


Figure 6. Potential distribution of *Dendrocopos major* in China predicted using the MaxEnt model under (a) the current climate and according to climate change in (b) 2050 and (c) 2090.

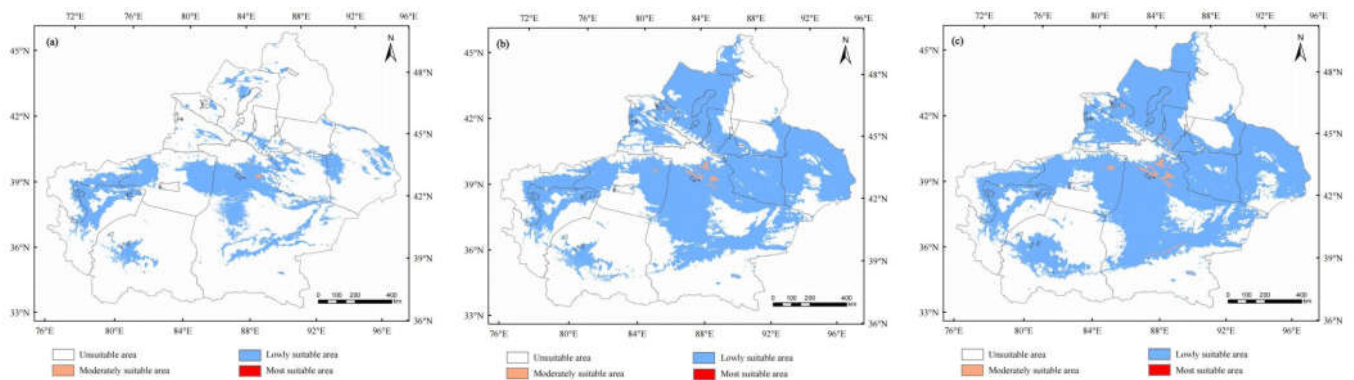


Figure 7. Potential distribution of *Dendrocopos major* in Xinjiang predicted using the MaxEnt model under (a) the current climate and according to climate change in (b) 2050 and (c) 2090.

3.2. Spatial transfer characteristics of suitable areas for ALB, *D. helophoroides*, and *D. major*

In China, from current conditions to 2050, the unsuitable area for ALB would decrease by 39.65×10^4 km², whereas the lowly suitable area, moderately suitable area, and most suitable area would increase by 14.96×10^4 , 14.87×10^4 , and 9.82×10^4 km², respectively (**Figure 8a**; **Figure S4a**). From 2050 to 2090, unsuitable and moderately suitable areas for ALB would decrease by 8.59×10^4 km² and 1.63×10^4 km², respectively, whereas the lowly suitable and most suitable areas would increase by 9.17×10^4 km² and 1.06×10^4 km², respectively (**Figure 8b**; **Figure S4a**). The centroid transfer trajectory from Yanan City (currently) to Dongsheng City (2050 and 2090) is shown in **Figure 8c**. From current conditions to 2050, the unsuitable area for ALB in Xinjiang would decrease by 16.33×10^4 km², whereas the lowly suitable area, moderately suitable area, and most suitable area would increase by 7.47×10^4 , 5.41×10^4 , and 3.45×10^4 km², respectively (**Figure 9a**; **Figure S4b**). From 2050 to 2090, the unsuitable area for ALB in Xinjiang would decrease by 4.81×10^4 km², whereas lowly, moderately, and most suitable areas would increase by 0.73×10^4 , 1.76×10^4 , and 2.32×10^4 km², respectively (**Figure 9b**; **Figure S4b**). The centroid transfer trajectory from Tarbagatay Prefecture (currently) to Shihezi City (2050) and Changji Hui Autonomous Prefecture (2090) is provided in **Figure 9c**.

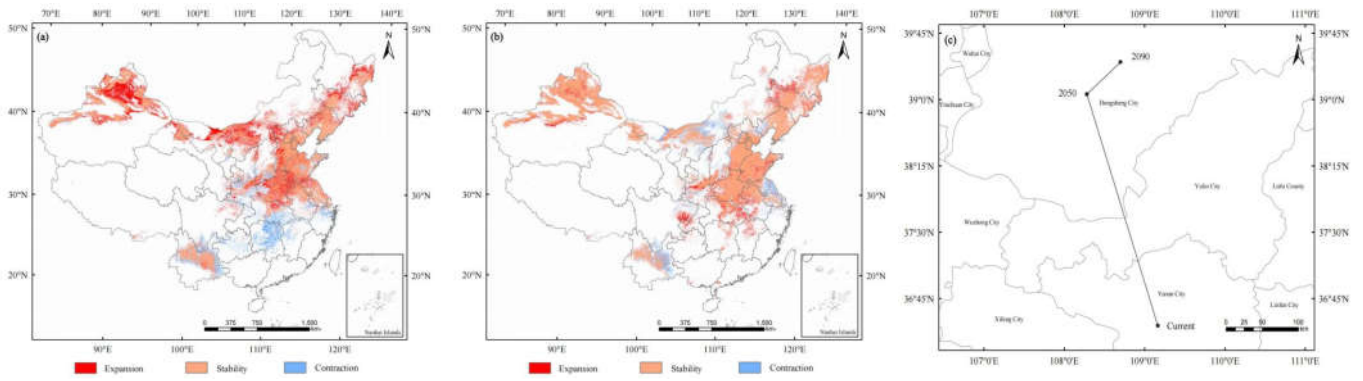


Figure 8. Spatial transfer characteristics of *Anoplophora glabripennis* in (a) current–2050 and (b) 2050–2090 stages and (c) centroid transfer trajectory in China.

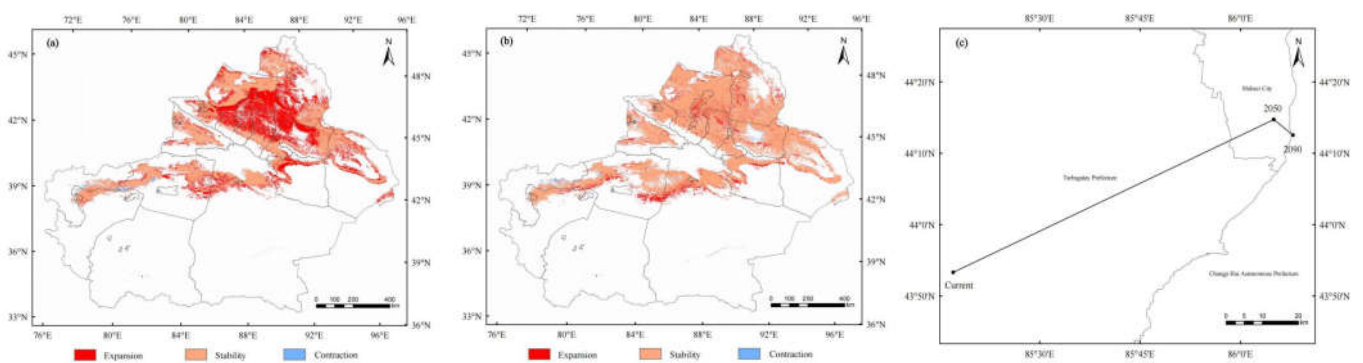


Figure 9. Spatial transfer characteristics of *Anoplophora glabripennis* in (a) current–2050 and (b) 2050–2090 stages and (c) centroid transfer trajectory in Xinjiang.

From current conditions to 2050, the unsuitable area for *D. helophoroides* in China would decrease by 101.22×10^4 km², whereas the lowly suitable area, moderately suitable area, and most suitable area would increase by 41.58×10^4 , 54.48×10^4 , and 5.16×10^4 km², respectively (**Figure 10a**; **Figure S4c**). From 2050 to 2090, the unsuitable area would decrease by 21.14×10^4 km², whereas the lowly suitable area, moderately suitable area, and most suitable area would increase by 3.34×10^4 , 13.82×10^4 , and 3.98×10^4 km², respectively (**Figure 10b**; **Figure S4c**). The centroid transfer trajectory from Weinan City (currently) to Yanan City (2050 and 2090) is provided in **Figure 10c**. From current conditions to 2050, the unsuitable area of *D. helophoroides* in Xinjiang would decrease by 42.64×10^4 km², whereas the lowly suitable area, moderately suitable area, and most suitable area would increase by 39.15×10^4 , 3.49×10^4 , and 0.000066×10^4 km², respectively (**Figure 11a**; **Figure S4d**). From 2050 to 2090, the unsuitable area would decrease by 7.49×10^4 km², whereas the lowly, moderately, and most suitable areas would increase by 1.96×10^4 , 5.52×10^4 , and 0.018×10^4 km², respectively (**Figure 11b**; **Figure S4d**). The centroid transfer trajectory from Luntai County (currently) to Kolar City (2050 and 2090) is provided in **Figure 11c**.

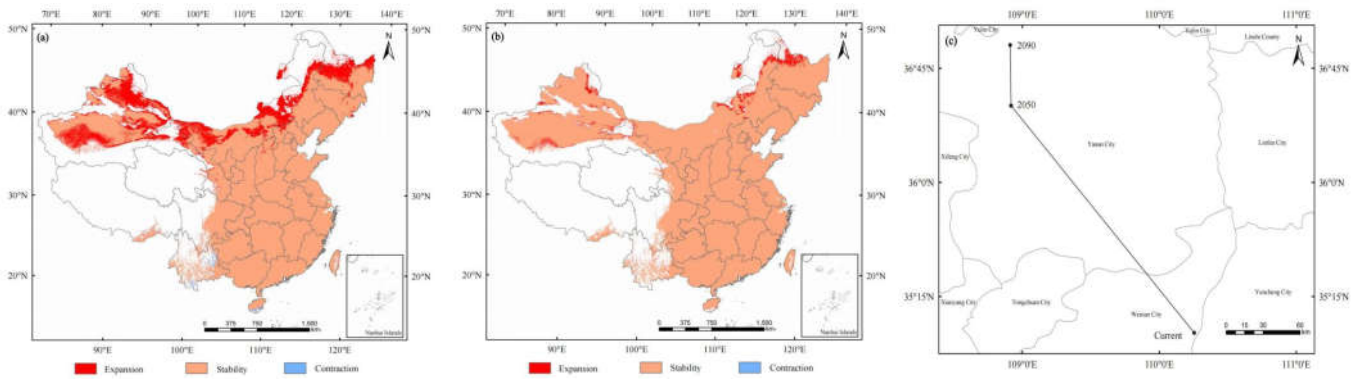


Figure 10. Spatial transfer characteristics of *Dastarcus helophoroides* in (a) current–2050 and (b) 2050–2090 stages and (c) centroid transfer trajectory in China.

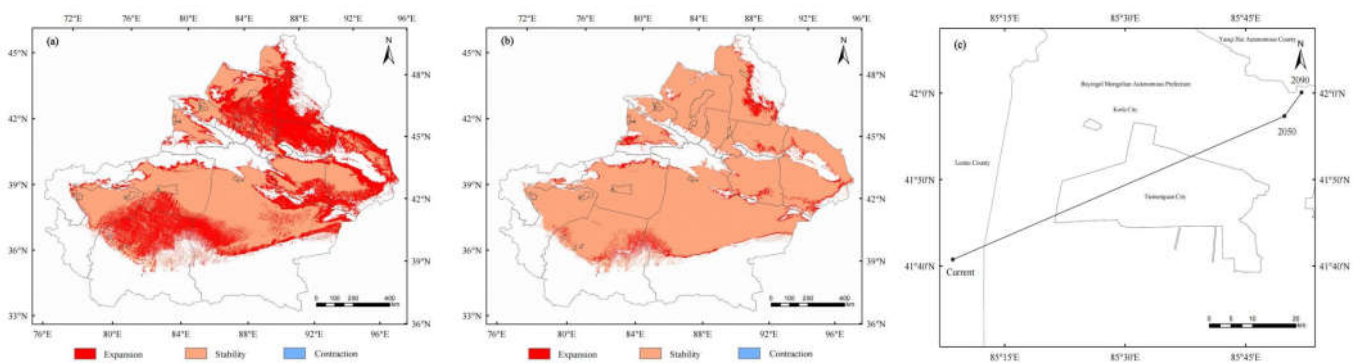


Figure 11. Spatial transfer characteristics of *Dastarcus helophoroides* in (a) current–2050 and (b) 2050–2090 stages and (c) centroid transfer trajectory in Xinjiang.

From current conditions to 2050, the unsuitable and most suitable areas of *D. major* would decrease by 110.59×10^4 and 29.04×10^4 km², respectively, whereas the lowly suitable and moderately suitable areas would increase by 75.37×10^4 and 64.26×10^4 km², respectively (Figure 12a; Figure S4e). From 2050 to 2090, the unsuitable, moderately suitable, and most suitable areas would decrease by 22.96×10^4 , 16.2×10^4 , and 20.25×10^4 km², respectively, whereas the lowly suitable area would increase by 59.40×10^4 km² (Figure 12b; Figure S4e). The centroid transfer trajectory from Xian City (currently) to Xifeng City (2050 and 2090) is provided in Figure 12c. From current conditions to 2050, the unsuitable area for *D. major* in Xinjiang would decrease by 50.05×10^4 km², whereas the lowly suitable and moderately suitable areas would increase by 49.62×10^4 and 0.43×10^4 km², respectively, with no most suitable area (Figure 13a; Figure S4f). From 2050 to 2090, the unsuitable area would decrease by 11.04×10^4 km², whereas the lowly suitable and moderately suitable areas would increase by 10.67×10^4 and 0.38×10^4 km², respectively, with no most suitable area (Figure 13b; Figure S4f). The centroid transfer trajectory from Qiemo County (currently) to (2050) and Yanqi Hui Autonomous County (2090) is provided in Figure 13c.

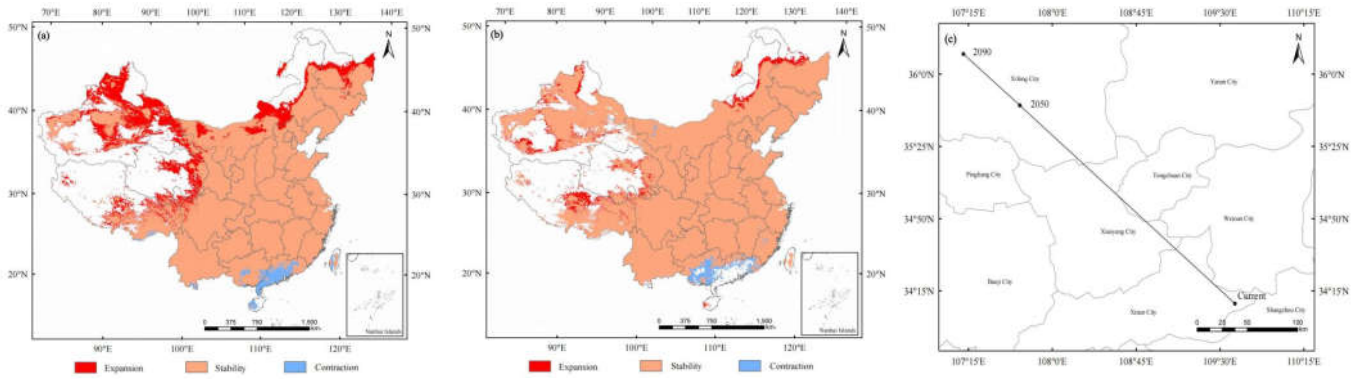


Figure 12. Spatial transfer characteristics of *Dendrocopos major* in (a) current–2050 and (b) 2050–2090 stages and (c) centroid transfer trajectory in China.

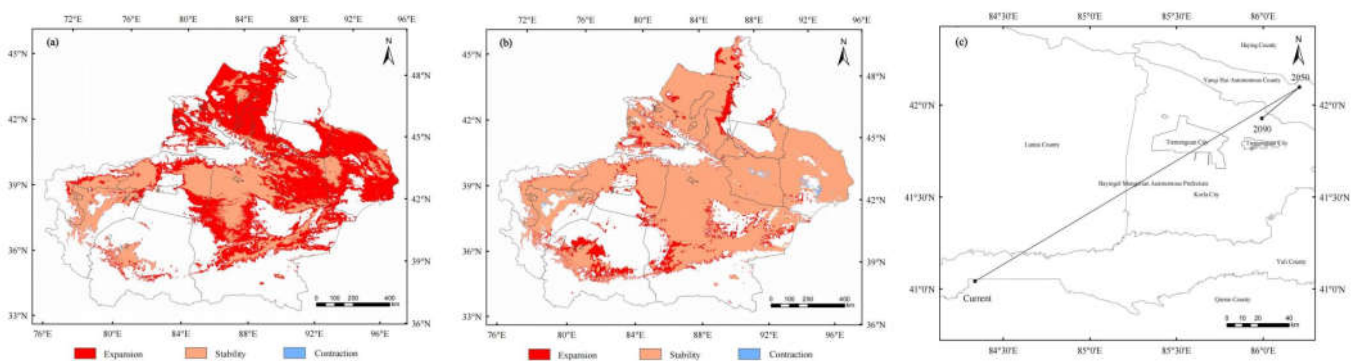


Figure 13. Spatial transfer characteristics of *Dendrocopos major* in (a) current–2050 and (b) 2050–2090 stages and (c) centroid transfer trajectory in Xinjiang.

3.3. The distribution overlap region of ALB, *D. helophoroides*, and *D. major*

In China, only the occurrence regions of ALB are distributed in parts of Xinjiang, Gansu, and Inner Mongolia. In other occurrence regions of ALB, control modes of ALB + *D. helophoroides*, ALB + *D. major*, or ALB + *D. helophoroides* + *D. major* were found (**Figure 14a**). In Xinjiang, the distribution of ALB mainly occurs in only northern Xinjiang, whereas ALB, *D. helophoroides*, and *D. major* all occur near the Tianshan Mountains (**Figure 14b**).

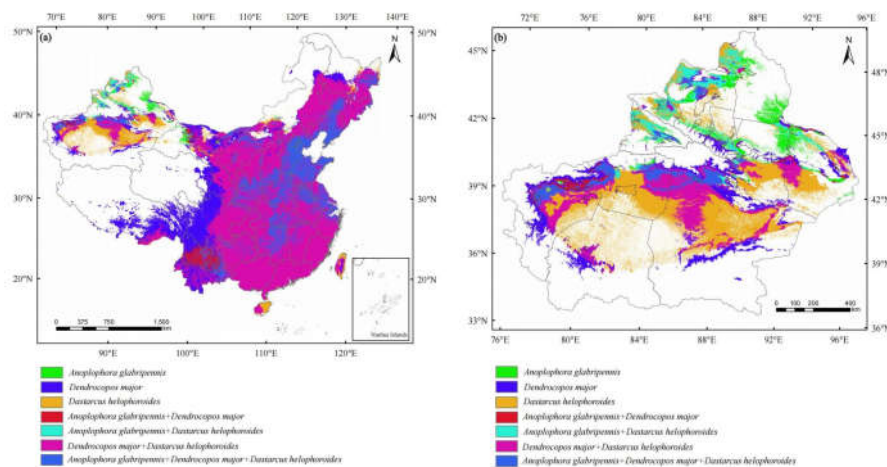


Figure 14. Prediction of overlapping suitable areas of *Anoplophora glabripennis*, *Dastarcus helophoroides*, and *Dendrocopos major* in (a) China and (b) Xinjiang.

4. Discussion

4.1. Reliability analysis of models established for ALB, *D. helophoroides*, and *D. major* by using MaxEnt

MaxEnt is widely used to predict the potential distribution area of invasive organisms [37], such as *Leptinotarsa decemlineata* [40], *Popillia japonica* [41], and *Sarconesia chlorogaster* [42]. These cases provide a more positive role for the management of invasive pests. In addition, CLIMEX, GARP, GIS, and other software are widely used to predict species distribution [43–44]. When compared with these software, MaxEnt can use the AUC value of the ROC curve to judge the prediction of the model [45], correct the sample deviation in the process of collecting known distribution data [46–47], and reduce spatial biases in the GBIF database for the geographical distribution of model species [48]. In this study, the established MaxEnt model was tested, and the ROC curve verification results for ALB, *D. helophoroides*, and *D. major* showed that the 10 repeated average values of AUC were 0.801 (Figure S5a), 0.838 (Figure S5b), and 0.828 (Figure S5c), respectively; these values were higher than the random AUC value (0.5) and close to 1.0, indicating that the constructed model was reliable and could be used to predict the distribution of ALB, *D. helophoroides*, and *D. major* in China and Xinjiang.

4.2. Contribution of environmental variables to the establishment of the MaxEnt model

Environmental variables play an important role in the establishment of species distribution models [49]. This is because climatic conditions affect the colonization, migration, growth, and reproduction of organisms [50–52]. Therefore, selection of appropriate environmental variables determines modeling accuracy [53]. Previous studies have shown that overwintering and distribution of ALB, *D. helophoroides*, and *D. major* are related to climatic factors such as temperature [54–57], and even the distribution of hosts was considered [58–59]. In this study, we used correlation analysis to screen for environmental variables useful for modeling and eliminated irrelevant factors bio5, bio7, bio8, bio9, bio17, and bio18 (Figure S6). The statistical results for the contribution rate showed that Bio15, Bio4, Bio1, Bio21, Bio12, Bio14, Bio2, Bio22, and Bio10 were the environmental factors that dominated the model for ALB suitable area (Figure S7a). Bio20, Bio6, Bio11, Bio12, Bio13, Bio22, Bio4, Bio3, Bio19, and Bio1 were the environmental factors that dominated the model for *D. helophoroides* suitable area (Figure S7b). Bio6, Bio11, Bio15, Bio4, Bio20, Bio3, Bio16, Bio19, Bio12, and Bio21 were the environmental factors that dominated the distribution model for *D. major* (Figure S7c). The Jackknife test showed that the training gain of annual mean temperature (Bio1) and standard deviation of seasonal temperature variation (Bio4) were higher than 0.6, which are key environmental variables that affect the distribution of ALB (Figure S8a). The training gain of minimum temperature (Bio6) and altitude (Bio20) in the coldest month were higher than 0.5, which are key variables that affect the distribution of *D. helophoroides* (Figure S8b). The training gain of the lowest temperature in the coldest month (Bio6) was the highest (>0.4), which is the key variable that affects the distribution of *D. major* (Figure S8c).

4.3. Sequential variations in the distribution of ALB, *D. helophoroides*, and *D. major* suitable areas under climatic conditions

Climate change is an important factor that affects species distribution and transfer [60]. The global temperature is gradually increasing, which directly leads to the northward migration of species in different climatic zones and opens up new habitats [61–62]. Among insects, *Chilo suppressalis* [63], *Drosophila melanogaster* [64], *Nezara viridula* [65], and *Bactrocera dorsalis* [66] have been confirmed to migrate northward with climate warming. Byeon [27] and Zhou [28] also showed that the climate suitability of ALB would increase in the region north of 30°N and decrease in most regions south of 30°N. Our results show that the suitable areas of ALB, *D. helophoroides*, and *D. major* continue to shift northward in the current–2050 and 2050–2090 stages, and suitable areas south of 30°N are gradually decreasing. These changes include the evolution of the most suitable area into moderately

suitable or lowly suitable area, evolution of moderately suitable area into lowly suitable area or unsuitable area, and evolution of lowly suitable area into unsuitable area. However, it is worrying that the latitude range of centroid transfer of ALB is larger than that of *D. helophoroides* and *D. major*. In China, the latitude range of the centroid transfer trajectory of *D. helophoroides* was 35°N–37°N (Figure 12c); *D. major*, 34°N–37°N (Figure 10c); and ALB, 36°N–40°N (Figure 8c). In Xinjiang, the latitude range of the centroid transfer trajectory of *D. helophoroides* was 41.40°N–42°N (Figure 13c); *D. major*, 41°N–42.20°N (Figure 11c); and ALB, 43.50°N–44.20°N (Figure 9c). These results indicate that the extent of invasion of ALB is greater than that of *D. helophoroides* and *D. major*. However, during the northward movement of ALB, the extent of the northward movement of natural enemies may not be able to keep up with that of ALB, leading to a reduction in the ability of the natural enemies to control ALB; this in turn may lead to an increase in the harm caused by ALB in the invaded areas.

4.4. Evaluation of the natural control ability of *D. helophoroides* and *D. major* against ALB on the basis of the MaxEnt model

We reviewed ecological models of suitable habitats for pests, and almost all studies only discussed the prediction of suitable habitats for single species under climatic conditions. It is worth noting that we need to re-evaluate these models from the perspective of pest control to assess whether natural enemy resources can be used to control invasive pests, which means that more than a single-species analysis is required. In this study, we superimposed the suitable areas of ALB and its important natural enemies, *D. helophoroides* and *D. major*, and found that, in most regions of China, niche overlaps exist between ALB and *D. helophoroides* and *D. major*, except for some regions in Xinjiang, Gansu, and Inner Mongolia (Figure 14). Thus, the areas with natural enemies tend to have low levels of damage, but ALB causes more serious damage in Xinjiang, Gansu, and Inner Mongolia [66-68]. These reports confirm that our model results are consistent with the actual phenomenon.

In addition, through literature and websites, we found that *D. helophoroides* exists in China, South Korea, Japan, and other regions [69-71]. *D. major* is distributed in Italy, France, the UK, Finland, the United States, Japan, the Korean Peninsula, and other countries or regions [72]. Perhaps these two natural enemies can be used in these countries or regions to control ALB. However, it should be noted that, during the process of introducing natural enemies, the safety of natural enemies in the introduction area should be carefully considered to avoid secondary invasion of natural enemies [73-74].

4.5. Use of MaxEnt model results for the management of ALB

Currently, chemical and biological control technologies are the main technical means used to effectively control the damage of ALB [75]. We consider that the use of MaxEnt simulation to predict the suitable area of natural enemies and ALB would be helpful to evaluate the prevention and control ability of natural enemies against ALB. If there are sustainably regulated natural enemies in the place of origin or invasion, then the natural enemies can be used to reduce the adverse effects of ALB. If there are no natural enemies in the place of origin or invasion, then natural enemies can be introduced scientifically and safely according to their suitability in the region. Although the natural control ability of natural enemies against ALB is decreasing with climate change, natural enemy regulation is a primitive way of regulating harmful organisms in nature and can reduce the use of chemicals. In the future, biological and chemical control can be appropriately combined to prevent large-scale deforestation and pesticide usage. This is of great significance for establishing the sustainable regulation of ALB.

Supplementary Materials:

Figure S1: Proportion of suitable area of *Anoplophora glabripennis* in (a–c) China and (d–e) Xinjiang;

Figure S2: Proportion of suitable area of *Dastarcus helophoroides* in (a–c) China and (d–e) Xinjiang;

Figure S3: Proportion of suitable area of *Dendrocopos major* in (a–c) China and (d–e) Xinjiang;

Figure S4: In current–2050 and 2050–2090 stages, suitable area changes of (a-b) *Anoplophora glabripennis*, (c-d) *Dastarcus helophoroides*, and (e-f) *Dendrocopos major* in China and Xinjiang;

Figure S5: ROC curve and AUC value for the MaxEnt model of (a) *Anoplophora glabripennis*, (b) *Dastarcus helophoroides*, and (c) *Dendrocopos major* distribution prediction;

Figure S6: Correlation analysis of environmental factors in the MaxEnt model;

Figure S7: Environmental variables used in the simulation for the distribution of potential suitable areas of (a) *Anoplophora glabripennis*, (b) *Dastarcus helophoroides*, and (c) *Dendrocopos major* and their percentage contributions;

Figure S8: Jackknife test for variable importance of (a) *Anoplophora glabripennis*, (b) *Dastarcus helophoroides*, and (c) *Dendrocopos major* suitability distribution;

Table S1: Environment variables for MaxEnt modeling;

Table S2: Environment variables for *Anoplophora glabripennis* distribution model

Table S3: Environment variables for *Dastarcus helophoroides* distribution model

Table S4: Environment variables for *Dendrocopos major* distribution model

Author Contributions: Q.Z. wrote the manuscript, processed the data, and created the figures for the manuscript. Y.L. participated in the investigation of the distribution of *Anoplophora glabripennis*, *Dastarcus helophoroides*, and *Dendrocopos major*, and J.W. reviewed the manuscript. All the authors have read and approved the final manuscript.

Funding: This research was supported by the Corps Forestry Bureau Project (KH0461) and the Corps Science and Technology Project (2019AB023).

Data Availability Statement: The data that support the findings of this study are available from the corresponding author upon reasonable request.

Acknowledgments: We thank Dr. Ya-Fei Qiao for help with MaxEnt mapping.

Conflicts of Interest: The authors declare no conflict of interest.

References

1. Haack, R.A.; Hérard, F.; Sun, J.H.; Turgeon, J.J. Managing invasive populations of Asian longhorned beetle and citrus longhorned beetle: a worldwide perspective. *Annu. Rev. Entomol.* **2010**, *55*, 521–546.
2. Lingafelter, S.W.; Hoebeke, E.R. Variation and homology in elytral maculation in the *Anoplophora malasiaca/macularia* species complex (Coleoptera : Cerambycidae) of Japan and Taiwan. *P. Entomol. Soc. Wash.* **2001**, *103*, 757–769.
3. Van der Gaag, D.; Loomans, A. Host plants of *Anoplophora glabripennis*, a review. *EPPO Bulletin* **2014**, *44*, 518–528.
4. Haack, R.A.; Cavey, J.F.; Hoebeke, E.R.; Law, K. *Anoplophora glabripennis*: a new tree-infesting exotic cerambycid invades New York. *Newsl. Michigan Entomol. Soc.* **1996**, *41*, 1–3.
5. Hérard, F., Ciampitti, M., Maspero, M., Krehan, H., Benker, U., Boegel, C., Schrage, R.; Bouhot-Delduc, L.; Bialooki, P. *Anoplophora* species in Europe: infestations and management processes. *EPPO Bulletin* **2006**, *36*, 470–474.
6. Turgeon, J.J.; Orr, M.; Grant, C.; Wu, Y.; Gasman, B. Decade-old satellite infestation of *Anoplophora glabripennis* Motschulsky (Coleoptera: Cerambycidae) found in Ontario, Canada outside regulated area of founder population. *Coleopterists Bull.* **2015**, *69*, 674–678.
7. Javal, M.; Lombaert, E.; Tsykun, T.; Courtin, C.; Kerdelhué, C.; Prospero, S.; Roques, A.; Roux, G. Deciphering the worldwide invasion of the Asian long-horned beetle: a recurrent invasion process from the native area together with a bridgehead effect. *Mol. Ecol.* **2019**, *28*, 951–967.
8. Yue, C.Y.; Zhang, X.P.; Liu, A.H.; Alimu, M. Risk analysis of the occurrence of *Anoplophora glabripennis* in Xinjiang. *J. Northwest For. Univ.* **2011**, *26*, 153–156.
9. Thomson, L.J.; Macfadyen, S.; Hoffmann, A.A. Predicting the effects of climate change on natural enemies of agricultural pests. *Biol. Control* **2010**, *52*, 296–306.
10. Hu, J.; Angeli, S.; Schuetz, S.; Luo, Y.; Hajek, A.E. Ecology and management of exotic and endemic Asian longhorned beetle *Anoplophora glabripennis*. *Agri. For. Entomol.* **2009**, *11*, 359–375.
11. Marchioro, M.; Faccoli, M. Successful eradication of the Asian longhorn beetle, *Anoplophora glabripennis*, from north-eastern Italy: protocol, techniques and results. *Insects* **2021**, *12*, 877.
12. Caltagirone, L.E. Landmark examples in classical biological control. *Annu. Rev. Entomol.* **1981**, *26*, 213–232.
13. Hufbauer, R.A.; Roderick, G.K. Microevolution in biological control: mechanisms, patterns, and processes. *Biol. Control* **2005**, *35*, 227–239.

14. Luo, L.P.; Wang, X.Y.; Yang, Z.Q.; Zhao, J.X.; Tang, Y.L. Progress in biological control over *Anoplophora glabripennis* (Coleoptera: Cerambycidae). *Biol. Dis. Sci.* **2018**, *41*, 247–255.
15. Yang, Z.Q.; Wang, X.Y.; Zhang, Y.N. Recent advances in biological control of important native and invasive forest pests in China. *Biol. Control* **2014**, *68*, 117–128.
16. Demidko, D.A.; Demidko, N.N.; Mikhaylov, P.V.; Sultson, S.M. Biological strategies of invasive bark beetles and borers species. *Insects* **2021**, *12*, 367–367.
17. Jiao, Z.B.; Wan, T.; Wen, J.B.; Hu, J.F.; Luo, Y.Q.; Zhang, L.S.; Fu, L.J. Functional response and numerical response of great spotted woodpecker *Dendrocopos major* on Asian longhorned beetle *Anoplophora glabripennis* larvae. *Acta Zool. Sin.* **2008**, *54*, 1106–1111.
18. Yue, C.Y.; Zhang, X.P.; Zhang, J.W.; Jiao, S.P.; Nuergu; Kereman; Han, X.W.; Ji, L.L. A preliminary study on the effect of release of *Dastarcus helophoroides* to control *Anoplophora glabripennis* in forest land of Yanqi Basin. *Xinjiang Agric. Sci.* **2013**, *50*, 2085–2091.
19. Wan, T.; Jiao, Z.B.; Wen, J.B.; Hu, J.F.; Luo, Y.Q.; Fu, L.J.; Zhang, L.S. Selective predation by the great spotted woodpecker *Dendrocopos major* on the Asian longhorned beetle *Anoplophora glabripennis* in winter. *Acta Zool. Sin.* **2008**, *54*, 555–560.
20. Lv, F.; Hai, X.X.; Wang, Z.G.; Liu, B.X.; Yan, A.H.; Bi, Y.G. Research progress in *Dastarcus helophoroides* Fairmaire (Bothrideridae), an important natural enemy of the longhorn beetle pests. *Sci. Sericul.* **2014**, *40*, 1107–1113.
21. Elith, J.; Phillips, S.J.; Hastie, T.; Dudík, M.; Chee, Y.E.; Yates, C.J. A statistical explanation of MaxEnt for ecologists. *Divers. Distrib.* **2011**, *17*, 43–57.
22. Petitpierre, B.; Kueffer, C.; Broennimann, O.; Randin, C.; Daehler, C.; Guisan, A. Climatic niche shifts are rare among terrestrial plant invaders. *Science* **2012**, *335*, 1344–1348.
23. MacLeod, A.; Evans, H.F.; Baker, R.H.A. An analysis of pest risk from an Asian longhorn beetle (*Anoplophora glabripennis*) to hardwood trees in the European community. *Crop Prot.* **2002**, *21*, 635–645.
24. Peterson, A.T.; Scachetti-Pereira, R. Potential geographic distribution of *Anoplophora glabripennis* (Coleoptera: Cerambycidae) in North America. *Am. Midl. Nat.* **2004**, *151*, 170–178.
25. Shatz, A.J.; Rogan, J.; Sangermano, F.; Miller, J.; Elmes, A. Modeling the risk of spread and establishment for Asian longhorned beetle (*Anoplophora glabripennis*) in Massachusetts from 2008–2009. *Geocarto Int.* **2016**, *31*, 813–831.
26. Pedlar, J.H.; McKenney, D.W.; Yemshanov, D.; Hope, E.S. Potential economic impacts of the Asian longhorned beetle (Coleoptera: Cerambycidae) in eastern Canada. *J. Econ. Entomol.* **2020**, *113*, 839–850.
27. Byeon, D.; Kim, S.; Jung, J.; Jung, S.; Kim, K.; Lee, W. Climate-based ensemble modelling to evaluate the global distribution of *Anoplophora glabripennis* (Motschulsky). *Agri. For. Entomol.* **2021**, *23*, 569–583.
28. Zhou, Y.T.; Ge, X.Z.; Zou, Y.; Guo, S.W.; Wang, T.; Zong, S.X. Prediction of the potential global distribution of the Asian longhorned beetle *Anoplophora glabripennis* (Coleoptera: Cerambycidae) under climate change. *Agri. For. Entomol.* **2021**, *23*, 557–568.
29. Wu, T.W.; Lu, Y.X.; Fang, Y.J.; Xin, X.G.; Li, L.; Li, W.P.; Jie, W.H.; Zhang, J.; Liu, Y.M.; Zhang, L.; Zhang, F.; Zhang, Y.W.; Wu, F.H.; Li, J.L.; Chu, M.; Wang, Z.Z.; Shi, X.L.; Liu, X.W.; Wei, M.; Huang, A.N.; Zhang, Y.C.; Liu, X.H. The Beijing climate center climate system model (BCC-CSM): the main progress from CMIP5 to CMIP6. *Geosci. Model Dev.* **2019**, *12*, 1573–600.
30. Fick, S.E.; Hijmans, R.J. WorldClim 2: new 1-km spatial resolution climate surfaces for global land areas. *Int. J. Climatol.* **2017**, *37*, 4302–4315.
31. Zhang, K.L.; Yao, L.J.; Meng, J.S.; Tao, J. Maxent modeling for predicting the potential geographical distribution of two peony species under climate change. *Sci. Total Environ.* **2018**, *634*, 1326–1334.
32. Li, D.X.; Li, Z.X.; Liu, Z.W.; Yang, Y.J.; Khoso, A.G.; Wang, L.; Deguang Liu. Climate change simulations revealed potentially drastic shifts in insect community structure and crop yields in China’s farmland. *J. Pest Sci.* **2022**. DOI: 10.1007/S10340-022-01479-3
33. Santana, P.A.; Kumar, L.; Da Silva, R.S.; Pereira, J.L.; Picanco, M.C. (2019) Assessing the impact of climate change on the worldwide distribution of *Dalbulus maidis* (DeLong) using MaxEnt. *Pest Manag. Sci.* **75**, 2706–2715.
34. Cobos, M.E.; Peterson, A.T.; Barve, N.; Osorio-Olvera, L. kuenm: an R package for detailed development of ecological niche models using Maxent. *PeerJ* **2019**, *7*, e6281.
35. Warren, D.L.; Seifert, S.N. Ecological niche modeling in Maxent: the importance of model complexity and the performance of model selection criteria. *Ecol. Appl.* **2011**, *21*, 335–342.
36. Peterson, A.T.; Soberón, J.; Pearson, R.G.; Anderson, R.P.; Martínez-Meyer, E.; Nakamura, M.; Araújo, M.B. Ecological niches and geographic distributions. Princeton University Press. **2011**.
37. Phillips, S.J.; Anderson, R.P.; Schapire, R.E. Maximum entropy modeling of species geographic distributions. *Ecol. Model.* **2006**, *190*, 231–259.
38. Phillips, S.J.; Anderson, R.P.; Dudík, M.; Schapire, R.E.; Blair, M.E. Opening the black box: an open-source release of Maxent. *Ecography* **2017**, *40*, 887–893.
39. Brown, J.L. SDM toolbox: a python-based GIS toolkit for landscape genetic, biogeographic and species distribution model analyses. *Methods Ecol. Evol.* **2014**, *5*, 694–700.
40. Wang, C.; Hawthorne, D.; Qin, Y.J.; Pan, X.B.; Li, Z.H.; Zhu, S.F. Impact of climate and host availability on future distribution of Colorado potato beetle. *Sci. Rep.* **2017**, *7*, 4489.
41. Zhu, G.P.; Li, H.Q.; Zhao, L. Incorporating anthropogenic variables into ecological niche modeling to predict areas of invasion of *Popillia japonica*. *J. Pest Sci.* **2017**, *90*, 151–160.

42. Lecheta, M.C.; Corrêa, R.C.; Moura, M.O. Climate shapes the geographic distribution of the blowfly *Sarconesia chlorogaster* (Diptera: Calliphoridae): An environmental niche modeling approach. *Environ. Entomol.* **2017**, *46*, 1051–1059.
43. Ge, X.Z.; Zong, S.X.; He, S.Y.; Liu, Y.T.; Kong, X.Q. Areas of China predicted to have a suitable climate for *Anoplophora chinensis* under a climate-warming scenario. *Entomol. Exp. Appl.* **2014**, *153*, 256–265.
44. Li, Z.H.; Qin, Y.J. Review on the quantitative assessment models for pest risk analysis and their comparison. *Plant Prot.* **2018**, *44*, 134–145.
45. Jimenez-Valverd, A. Insights into the area under the receiver operating characteristic curve (AUC) as a discrimination measure in species distribution modelling. *Global Ecol. Biogeogr.* **2012**, *21*, 498–507.
46. Kramer-Schadt, S.; Niedballa, J.; Pilgrim, J.D.; Schröder, B.; Lindenborn, J.; Reinfelder, V.; Stillfried, M.; Heckmann, I.; Scharf, A.K.; Augeri, D.M.; Cheyne, S.M.; Hearn, A.J.; Ross, J.; Macdonald, D.W.; Mathai, J.; Eaton, J.; Marshall, A.J.; Semiadi, G.; Rustam, R.; Bernard, H.; Alfred, R.; Samejima, H.; Duckworth, J.W.; Breitenmoser-Wuersten, C.; Belant, J.L.; Hofer, H.; Wilting, A. (2013) The importance of correcting for sampling bias in MaxEnt species distribution models. *Divers. Distribut.* **19**, 1366–1379.
47. Syfert, M.M.; Smith, M.J.; Coomes, D.A. The effects of sampling bias and model complexity on the predictive performance of MaxEnt species distribution models. *PLoS ONE*, **2013**, *8*, e55158.
48. Beck, J.; Böller, M.; Erhardt, A.; Schwanghart, W. Spatial bias in the GBIF database and its effect on modeling species' geographic distributions. *Ecol. Inform.* **2014**, *19*, 10–15.
49. Li J.L.; Tang, X.Q. The research progress on assessment model of ecosystem under global climate change. *Grassland Turf* **2014**, *34*, 86–93.
50. Ward, N.L.; Masters, G.J. Linking Climate change and species invasion: an illustration using insect herbivores. *Global Change Biol.* **2007**, *13*, 1605–1615.
51. Ghini, R.; Hamada, E.; Pedro Junior, M.J.; Marengo, J.A.; Goncalves, R.R. Risk analysis of climate change on coffee nematodes and leaf miner in Brazil. *Pesqui. Agropecu. Bras.* **2008**, *43*, 187–194.
52. Gomi, T.; Nagasaka, M.; Fukuda, T.; Hagihara, H. Shifting of the life cycle and life-history traits of the fall webworm in relation to climate change. *Entomol. Exp. Appl.* **2007**, *125*, 179–184.
53. Chen, Y.; Ma, C.S. Effect of global warming on insect: a literature review. *Acta Ecol. Sin.* **2010**, *30*, 2159–2172.
54. Feng, Y.Q.; Xu, L.L.; Tian, B.; Tao, J.; Wang, J.L.; Zong, S.X. Cold hardiness of Asian longhorned beetle (*Anoplophora glabripennis*) larvae in different populations. *Environ. Entomol.* **2014**, *43*, 1419–1426.
55. Feng, Y.Q., Xu, L.L., Li, W.B., Xu, Z.C., Cao, M., Wang, J.L., Tao, J.; Zong, S.X. Seasonal changes in supercooling capacity and major cryoprotectants of overwintering Asian longhorned beetle (*Anoplophora glabripennis*) larvae. *Agri. For. Entomol.* **2016a**, *18*, 302–312.
56. Wei, J.R.; Wang, S.Y.; Niu, Y.L.; Tang, Y.L. Cold tolerance of *Dastarcus helophoroides*. *For. Pest Dis.* **2010**, *29*, 19–20, 46.
57. Wei, K.; Zhang, Y.N.; Yang, Z.Q.; Wang, X.Y.; Han, Y.Y.; Liu, Y.; Qu, M.Q. Overwintering and cold tolerance of a parasitic natural enemy, *Dastarcus helophoroides* (Coleoptera: Bothrideridae), in Gansu Province. *For. Res.* **2015**, *28*, 588–592.
58. Feng, Y.Q.; Tursun, R.; Xu, Z.C.; Ou-Yang, F.; Zong, S.X. Effect of three species of host tree on the cold hardiness of overwintering larvae of *Anoplophora glabripennis* (Coleoptera: Cerambycidae). *Eur. J. Entomol.* **2016b**, *113*, 212–216.
59. Rong, K.; Si, Y.H.; Pan, Q.Y.; Wang, H. Forage niche differentiation of three sympatric woodpecker species in winter. *Acta Ecol. Sin.* **2018**, *38*, 8314–8323.
60. Hickling, R.; David, B.R.; Jane, K.H.; Chris, D.T. A northward shift of range margins in *British Odonata*. *Global Change Biol.* **2005**, *11*, 502–506.
61. Speight, M.R.; Hunter, M.D.; Watt, A.D. Ecology of Insects: Concepts and Applications. Blackwell Science Ltd, Oxford. **1999**.
62. Broadmeadow, M. Climate change: impacts on UK forests. Bulletin 125. Forestry Commission, Edinburgh. **2002**.
63. Morimoto, N.; Imura, O.; Kiura, T. Potential effects of global warming on the occurrence of Japanese pest insects. *Appl. Entomol. Zool.* **1998**, *33*, 147–155.
64. Umina, P.A.; Weeks, A.R.; Kearney, M.R.; McKechnie, S.W.; Hoffmann, A.A. A rapid shift in a classic clinal pattern in *Drosophila* reflecting climate change. *Science* **2005**, *308*, 691–693.
65. Musolin, D.L. Insects in a warmer world: ecological, physiological and life-history responses of true bugs (Heteroptera) to climate change. *Global Change Biol.* **2007**, *13*, 1565–1585.
66. Stephens, A.E.A.; Kriticos, D.J.; Leriche, A. The current and future potential geographical distribution of the oriental fruit fly, *Bactrocera dorsalis* (Diptera: Tephritidae). *B. Entomol. Res.* **2007**, *97*, 369–378.
67. Wang, Z.; Yuan, K.Y.; Wang, X.M. Investigation of damages and annual life history of *Anoplophora glabripennis* (Motsch.) in Baotou in the Inner Mongolia Autonomous region. *J. Inner Mongolia Agric. Univ.* **2016**, *37*, 87–96.
68. Ma, L.L. Study on the insect monitoring and control techniques of *Anoplophora glabripennis* and *Myzus persicae* in Lanzhou Lanshan area. *Gansu Forest* **2021**, *1*: 43–44.
69. Ogura, N.; Tabata, K.; Wang, W. Rearing of the colydiid beetle predator, *Dastarcus helophoroides*, on artificial diet. *BioControl* **1999**, *44*, 291–299.
70. Togashi, K.; Itabashi, M. Maternal size dependency of ovariole number in *Dastarcus helophoroides* (Coleoptera: Colydiidae). *J. Forest Res.* **2005**, *10*, 373–376.
71. Lim, J.; Oh, H.; Park, S.; Koh, S.; Lee, S. First record of the family Bothrideridae (Coleoptera) in Korea represented by the wood-boring beetle ectoparasite, *Dastarcus helophoroides*. *J. Asia-Pacific Entomol.* **2012**, *15*, 273–275.
72. GBIF. <https://www.gbif.org>

-
73. Gould, J.R.; Aflague, B.; Murphy, T.C.; McCartin, L.; Elkinton, J.S.; Rim, K.; Duan J.J. Collecting nontarget wood-boring insects for host-specificity testing of natural enemies of Cerambycids: A case study of *Dastarcus helophoroides* (Coleoptera: Bothriideridae), a parasitoid of the Asian longhorned beetle (Coleoptera: Cerambycidae). *Environ. Entomol.* **2018**, *47*, 1440–1450.
 74. Rim, K.; Golec J.R.; Duan, J.J. Host selection and potential non-target risk of *Dastarcus helophoroides* , a larval parasitoid of the Asian longhorned beetle, *Anoplophora glabripennis*. *Biol. Control* **2018**, *123*, 120–126.
 75. Li H.P.; Lv, F.; Bi, Y.G.; Wang, Z.G. Reviews on the serious wood-boring pest *Anoplophora glabripennis* in forestry of China. *For. Ecol. Sci.* **2020**, *35*, 1–9.